Various Coil Configurations Used in Coreless Motors

Clyde Hancock

Introduction

There exists a type of DC motor known as a coreless or slotless motor. The main feature of this type of motor is the fact that there is no iron (core) associated with the coil. This means that there are no iron losses; no cogging torque; the inductance is lower than that of typical iron cored motors (less sparking of the commutator); the rotor mass is lower so they have very high acceleration rates; and they are excellent for low-voltage operation when using precious metal brushes. These motors are typically around 1 mm to 70 mm in diameter. These motors are found in pagers, medical devices (i.e. — insulin pumps), pick-and-place robotics and more. There are many different coreless coils available today for both mechanical and electrically commutated DC motors. A few are pictured in the appendix at the end of this paper. This paper will investigate several coreless coils. This investigation is limited to radial gap devices. Three-dimensional finite element analysis (FEA) simulation as well as research from published information is used to compare the features of the various coil configurations.

I have been involved with the design and application of motors and generators for the past thirty nine years. Throughout this period, I have been asked about the advantage of one style of coreless coil as compared to another. Which one is the best? On the surface, this seems to be a question with a rather simple answer. Coil A is better than coil B, C, or D, etc. However, this is not the case; the criteria used to judge the merit of one coil versus another is instrumental in making a valid decision. A list of items to consider for the comparison includes, but is not limited to, the magnetic circuit, copper density, end turn losses, and ease of manufacturing. All of these items contribute to the overall quality of the design, and each style may have advantages based solely on an individual attribute.

In the next section (II), a variety of coils are described and a computer model of each is developed for analysis. In Section III, an approach for comparison of coils based on catalog information is presented. Section IV consists of the results from FEA and catalog comparisons. Section V summarizes what has been done in this analysis and conclusions presented based on the results, as well as suggestions for future research.

Coil Decriptions and FEA Models

This investigation compares six coil styles (Fig. 1); Faulhaber, hexagon, rhombic, parallel, multiple Saddle, and Saddle. The first four are constructed using the "combined turn coil" method provided by the FEA software (Figs. 2-5). This feature allows the user to describe the coil by individual arcs, segments, and dimensions. The last two use built-in coil geometries available in the FEA software (Figs. 6-7). The geometric shape is fixed, while the dimensions are defined by geometric parameters. Inside and outside diameter of the coils are the same. The lengths of the coils constructed via the "combined turn coil" method are the same and represent the axial length of the magnet. The saddle style coils provided by the FEA software have end turn length extending past the axial length of the magnet. First the coils are modeled without permanent magnets or steel. The coils are energized with DC current that is arranged as a three-phase delta connection. Post-processing cylinders are constructed for the inside, center, and outside diameters of the coils; this allows the viewing of the fields generated by the coils themselves. Next, a diametrically magnetized two-pole permanent magnet is added to the inside diameter of the coil with a steel ring added to the outside diameter of the coil (Fig. 8). The coil has a radial air gap on each side. A torque profile is constructed by rotating the permanent magnet with respect to the energized coil for 360º in 10º increments and solving for the torque developed at each position.

The Faulhaber coil is unique in that it is a complete freestanding coil after the winding process is complete. The first half-turn of the Faulhaber coil traverses the full length of the winding in an oblique direction through 180° of rotation. The second half returns the length of the winding through another 180° of rotation (Figs. 1A and 2A). The remaining turns are indexed and wound to form a complete coil (Fig. 2B). Loops (not shown) are pulled at the end of the coil during the winding process in intervals that correspond to the separate segments or phases.

The remaining coils in this comparison require additional steps to achieve the final cylindrical shape. The hexagon, rhombic and parallel coils (Figs. 1B, 1C, 1D, 3A, 4A and 5A) are wound on a mandrel that establishes the shape of the coil, i.e. — hexagon, lozenge or diamond, and rectangle, respectfully. After the winding is completed, the coil is removed from the mandrel, flattened, and rolled into a coil (Figs. 3B-5B). Loops (not shown) are pulled for segments or phases, as in the Faulhaber coil.

The saddle and multi-saddle coils are wound as individual coil sections (Figs. 1E, 1F, 6A, and 7A). After winding, the coil sections are formed and placed in position for the final coil assembly (Figs. 6B-7B). Each coil has a start and finish that must be interconnected with the appropriate coils to establish the segments or phases.

In all cases, the coil inside diameter, outside diameter, number of turns, and applied current are the same.

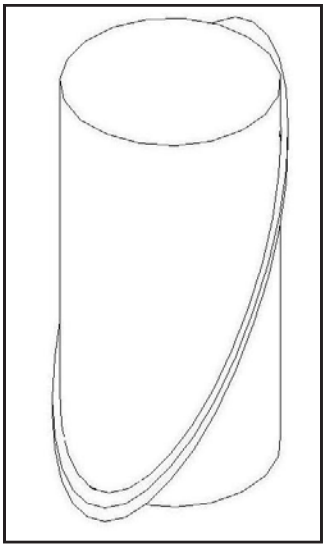

Figure 1A Faulhaber Coil.

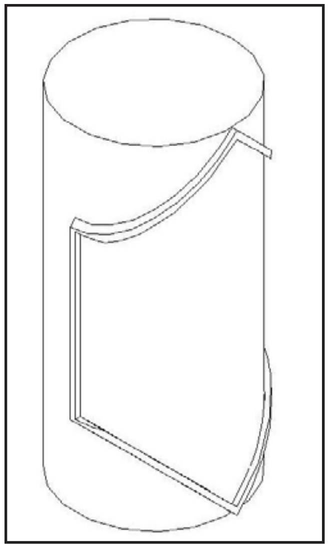

Figure 1B Hexagon Coil.

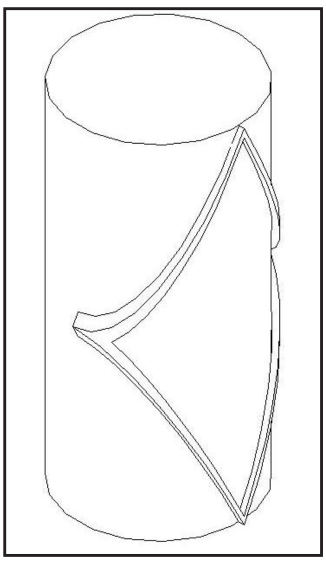

Figure 1C Rhombic Coil.

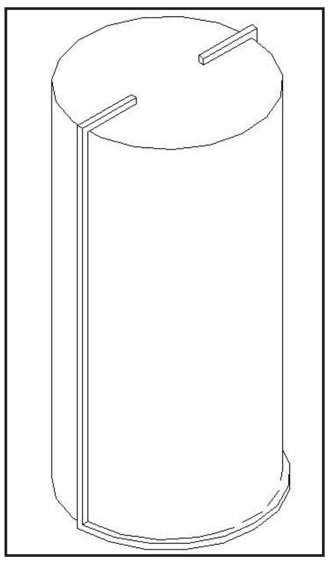

Figure 1D Parallel Coil.

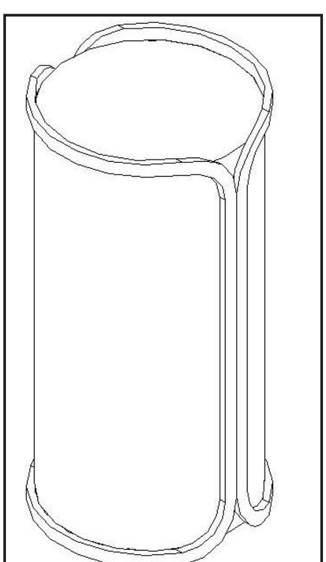

Figure 1E Multiple Saddle Coil.

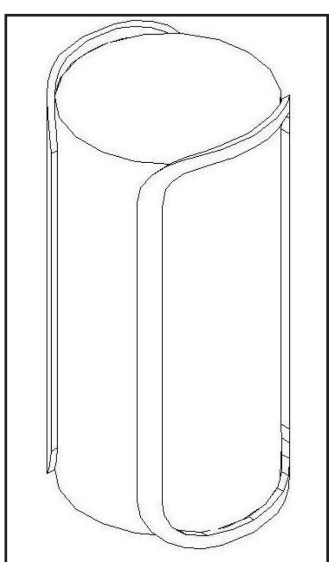

Figure 1F Saddle Coil.

Figure 1 Various Coil Shapes.

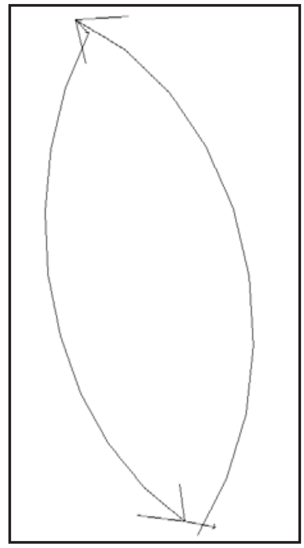

Figure 2A Single Turn of Faulhaber Coil.

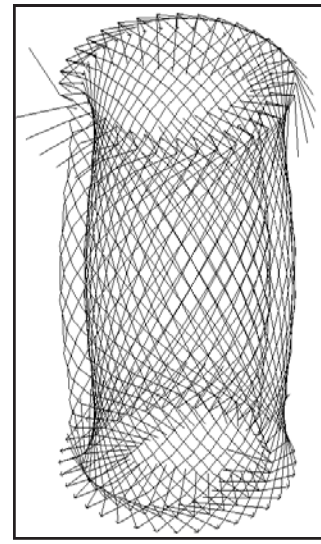

Figure 2B Complete Faulhaber Coil.

Figure 2 FEA Model of Faulhaber Coil.

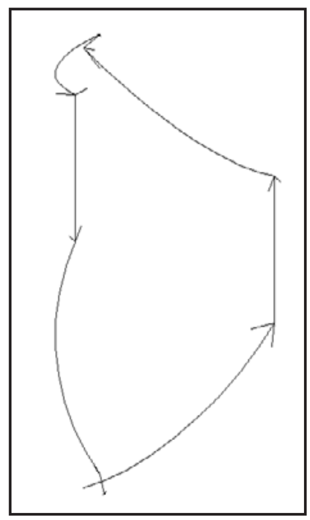

Figure 3A Single Turn of Hexagon Coil.

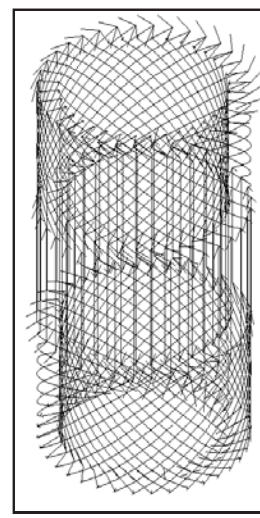

Figure 3B Complete Hexagon Coil.

Figure 3 FEA Model of Hexagon Coi

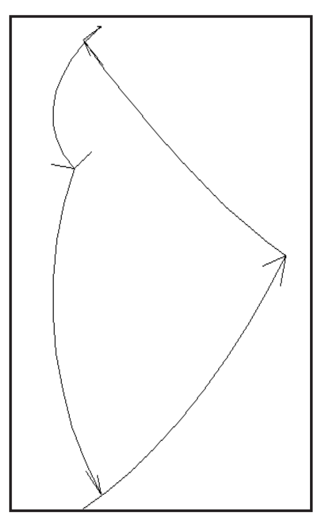

Figure 4A Single Turn of Rhombic Coil.

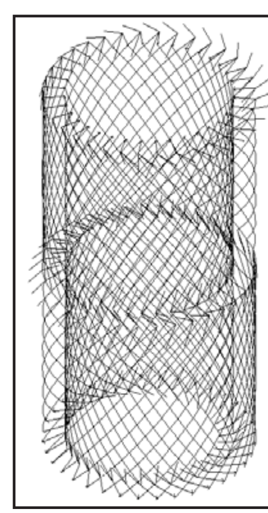

Figure 4B Complete Rhombic Coil.

Figure 4 FEA Model of Rhombic Coil.

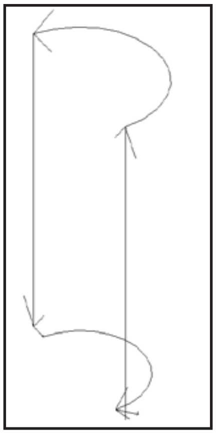

Figure 5A Single Turn of Parallel Coil.

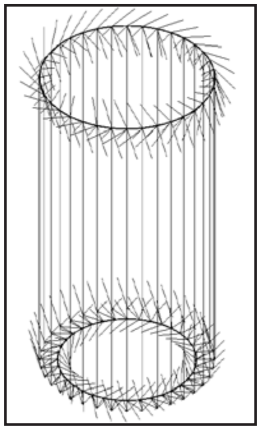

Figure 5B Complete Parallel Coil.

Figure 5 FEA Model of Parallel Coil

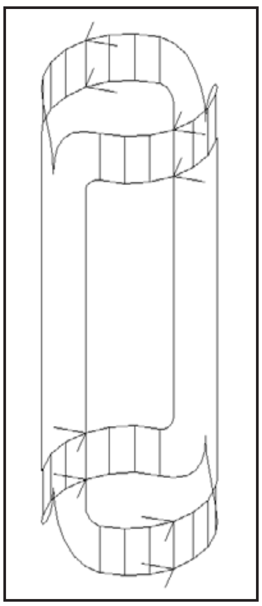

Figure 6A Single Phase of Multiple Saddle Coil.

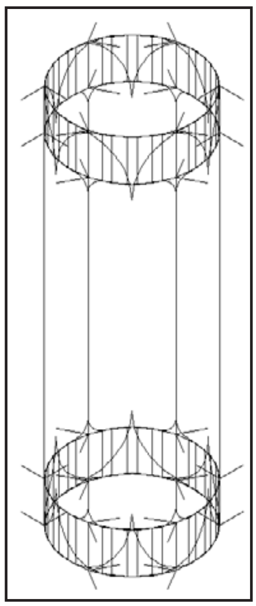

Figure 6B Complete Multiple Saddle Coil.

Figure 6 FEA Model of Multiple Saddle Coil.

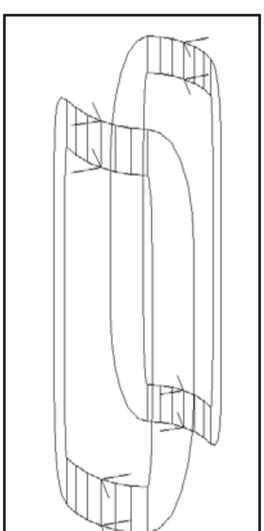

Figure 7A Single Phase of Saddle Coil.

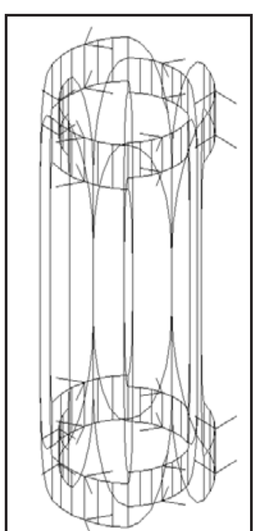

Figure 7B Complete Saddle Coil.

Figure 7 FEA Model of Saddle Coil.

Catalog Data Comparison

A comparison of catalog data is interesting — though not conclusive. The data published in the catalog does not detail the inner workings of the motors. The number of turns, the dimensions, and the diameter of the wire used in making the coil are not published. In addition, the material, size, and grade of the magnet are unknown. Two coil styles are readily compared, i.e. — the Faulhaber and the rhombic. Some manufacturers do not publish the type of coil that they employ in their product. Moreover, the size and power of motors manufactured using the various coils are not always comparable. The Faulhaber coil was patented and is used by several manufacturers with published data. The method of producing the hexagon coil was patented by Eastman Kodak and the rhombic coil is used by at least one manufacturer with published data.

A motor size is chosen to establish a common ground for comparison. The length and diameter as published in the catalog should match as closely as possible. Next, the winding constant is considered and matched accordingly. This establishes motors from different manufacturers with equivalent torque-per-amp-per-volume. The parameters for comparison include resistance, inductance, maximum power, and thermal resistance.

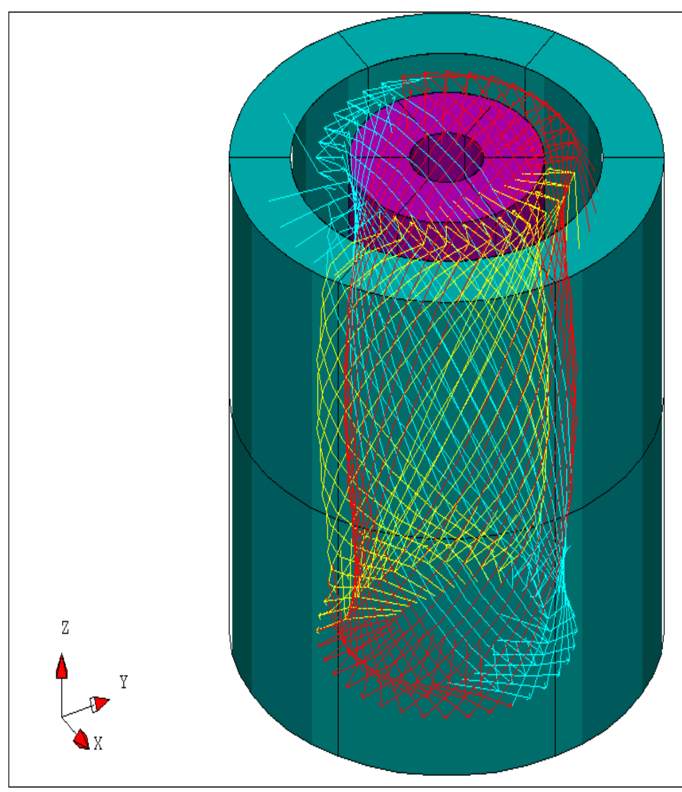

Figure 8 Example of Complete Model for the Faulhaber Coil

- Magnet Inside Diameter: 4.87 Mm
- Magnet Outside Diameter: 12.87 Mm
- Coil Inside Diameter: 13.55 Mm
- Coil Outside Diameter: 17.15 Mm
- Steel Return Inside Diameter: 20.58 Mm
- Steel Return Outside Diameter: 28.58mm
- Axial Length: 27mm

Results of FEA and Catalog Comparison

Results generated by the FEA comparison for the coils alone are viewed in the post processor. A relief map of the inner and outer diameter depicts the intensity and shape of the magnetic flux density in the theta direction using the cylindrical coordinate system *R*, θ, and *Z* (Figs. 9-14). The magnetic flux density in Tesla is represented by color on the scale to the right. The relief map shows the per-unit axial length of the post-processing cylinders on the *y* axis, and the per-unit circumference on the *x* axis. Interpretation of the relief maps is somewhat subjective. The relief maps afford the ability to see the relative shapes and intensity of magnetic flux density for the various coil geometries.

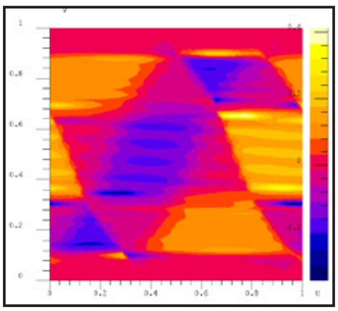

Figure 9A Faulhaber Coil ID Magnetic Flux Density.

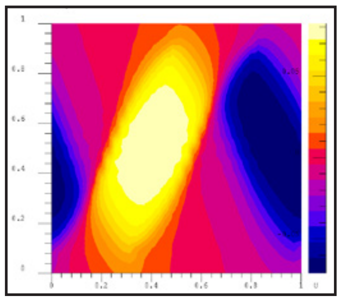

Figure 9B Faulhaber Coil OD Magnetic Flux Density.

Figure 9 Magnetic Flux Density in θ Direction for the Faulhaber Coil.

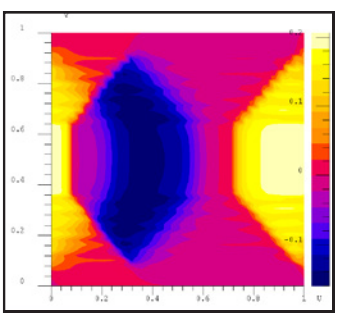

Figure 10A Hexagon ID Magnetic Flux Density.

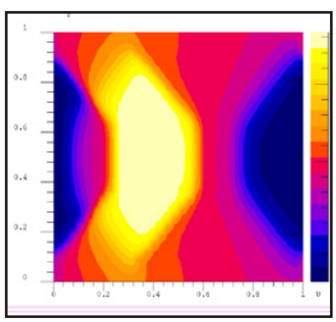

Figure 10B Hexagon OD Magnetic Flux Density.

Figure 10 Magnetic Flux Density in θ Direction for the Hexagon Coil.

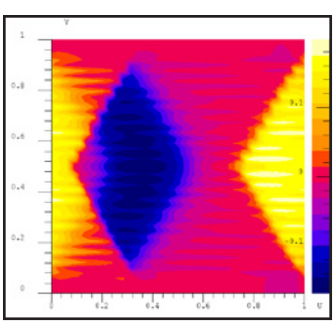

Figure 11A Rhombic ID Magnetic Flux Density.

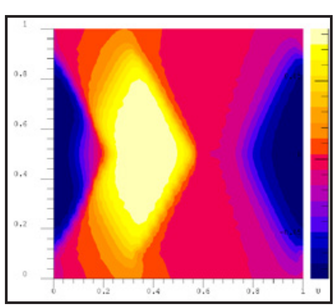

Figure 11B Rhombic OD Magnetic Flux Density.

Figure 11 Magnetic Flux Density in θ Direction for the Rhombic Coil.

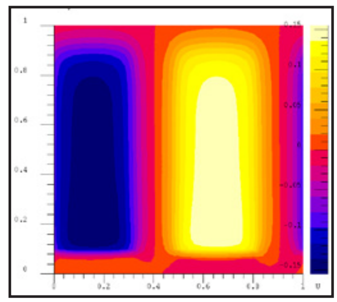

Figure 12A Parallel ID Magnetic Flux Density.

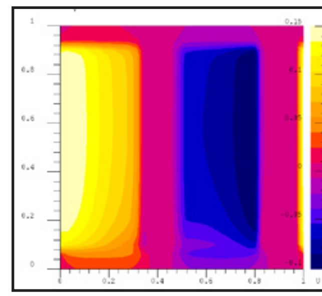

Figure 12B Parallel OD Magnetic Flux Density.

Figure 12 Magnetic Flux Density in θ Direction for the Parallel Coil.

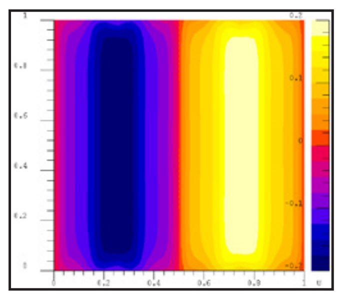

Figure 13A Multiple Saddle ID Magnetic Flux Density.

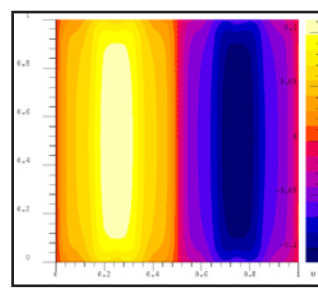

Figure 13B Multiple Saddle OD Magnetic Flux Density.

Figure 13 Magnetic Flux Density in θ Direction for the Multiple Saddle Coil.

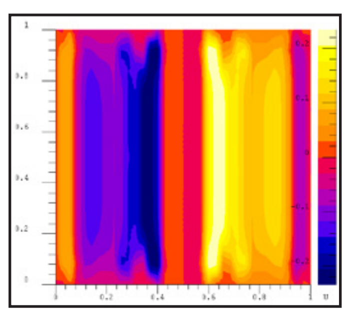

Figure 14A Saddle ID Magnetic Flux Density.

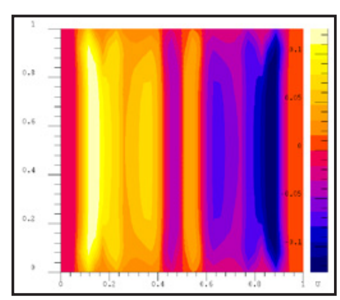

Figure 14B Saddle OD Magnetic Flux Density.

Figure 14 Magnetic Flux Density in θ Direction for the Saddle Coil.

The results of the torque profiles generated by the FEA models are represented (Fig. 15). The graph depicts the torque for each of the coil styles studied. The values on the graph's *y* axis represent the measured torque between the stationary portions (coil and steel return) and the rotated portion (magnet) in 10° increments for one full revolution; the current and number of turns are the same for each coil.

Table 1 shows comparisons for manufacturers "A" vs. "B" and "A" vs. "C". Manufacturers "A" and "C" are Faulhaber coils; manufacturer "B" is a rhombic coil. In all cases, the motors being compared have the same outside diameter. The lengths were selected to be as close as possible; however they vary in some cases. In the column labeled K_T, the shaded area colors match for the motor being evaluated. The column labeled $P_{2\,max.}$ is calculated with the recommended nominal voltage, resistance, and no-load current.

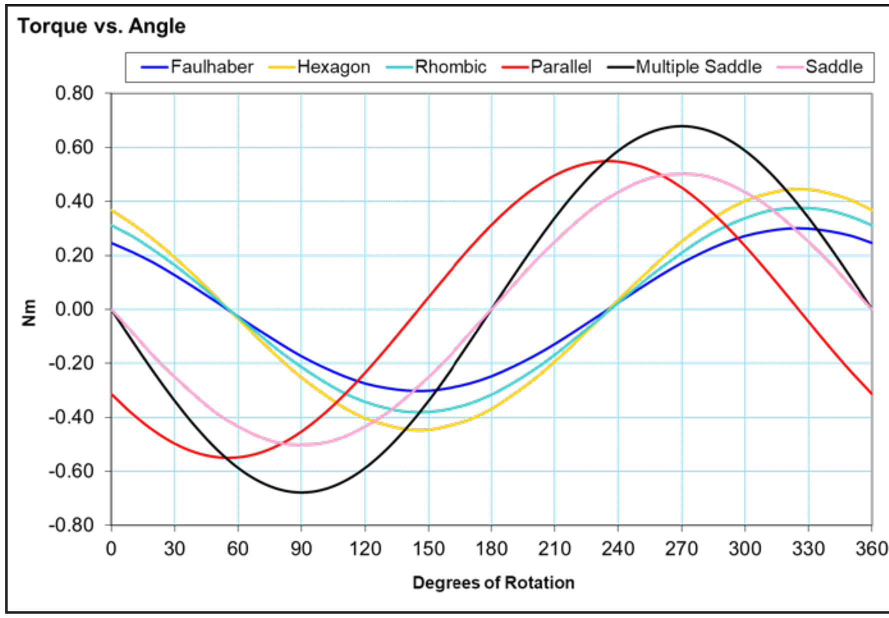

Figure 15 Torque vs rotor position.

Table 1 Comparison of Published Catalog Data for Manufacturers A, B, & C

Manufacturer	Diameter mm	Length mm	Nominal Voltage	Speed NL RPM	KT Nmm/A	R W	L mH	Rth 1 °C/W	Rth 2 °C/W	KM Nmm/√Watts	INL A	P2 max. Watts
A	15	23.8	6	9700	5.8	5.1	0.070	4.5	31	2.568	0.021	1.702
			9	10100	8.37	10.4	0.150			2.595	0.014	1.885
			12	9900	11.4	19.8	0.250			2.56	0.011	1.753
			18	9900	17.1	44	0.560			2.58	0.007	1.778
			24	9900	22.8	79.6	1.000			2.56	0.005	1.750
B	15	22.3	4.5	7450	5.62	6.46	0.120	8.2	35	2.21	0.017	0.746
			7.2	7740	8.67	15.3	0.290			2.22	0.011	0.808
			9	7710	10.9	24.4	0.460			2.21	0.009	0.790
			15	8110	17.2	62.2	1.150			2.18	0.006	0.860
			24	9890	22.7	109	1.990			2.17	0.005	1.262
A	26	57	12	6300	17.3	0.79	0.095	1.9	9	19.46	0.116	44.876
			24	6400	34.8	3.2	0.380			19.45	0.058	44.307
B	26	58.8	18	9910	17.1	1.52	0.100	4.2	9.7	13.87	0.061	52.742
			36	10300	33.1	4.72	0.360			15.24	0.032	68.069
			36	9400	36.3	5.68	0.430			15.23	0.028	56.539
A	17	24	6	8600	6.61	3.41	0.075	4	24.5	3.58	0.023	2.571
C	17	25.9	6	8500	6.7	3.2	0.110	10	30	3.75	0.011	2.781
A	22	32.6	18	8700	19.6	25	0.600	4	27	3.92	0.007	3.177
C	22	32	12	5900	19.3	27	1.200	6	22	3.71	0.004	1.312
A	26	42	24	6400	34.6	5.78	0.550	2.1	11	14.39	0.058	24.222
C	26	42	24	6700	33.5	32	1.700	5	12	5.92	0.012	4.357
A	28	42	12	5100	22	5.3	0.580	2	16	9.56	0.050	6.496
			24	5000	44.8	21	2.500			9.78	0.025	6.560
C	28	42	12	5300	21.4	5.95	0.500	5	12	8.77	0.022	5.919
			24	5600	40.7	19.5	2.400			9.22	0.011	7.253

Conclusions

Based strictly on the FEA analysis, it is clear that there is an electromagnetic advantage to winding coils with certain geometric features. What is not readily apparent from the evaluation of a single conductor in a magnetic field is the overall effect of the geometry for a complete coil. The interaction of the conductors assembled as a coil would indeed be difficult to imagine without the use of tools that simulate the device in three dimensions. I believe that, although subjective due to scaling, the relief maps indicate preferred geometries for optimizing coils. The torque observed for the various coils also demonstrate that there are preferred geometries.

The comparisons of catalog data are minimal; they indicate that there is more than just a difference in the coil shape. Alternative methods of fabricating the coil are a factor. As seen in Table 1, Manufacturer "A" motors are consistently lower in the reported coil thermal resistance ($R_{th\,1}$) than either "B" or "C" motors. After disassembling samples of the motors, it was noted that both "B" and "C" motors use some sort of wrapping on the outside diameter of the coils. This of course acts as insulation. This would leave less room for copper (smaller-diameter wire) or require larger air gaps. This may account for the higher resistance seen in the table.

This study, although interesting, is not conclusive. Much more work could be done in areas such as length-to- diameter ratio effects, state of the art winding techniques, and the number of permanent magnet poles with respect to the number of coil segments or phases.

If your application requires high acceleration, low sparking, zero cogging, and no eddy current loss, then you should consider the coreless DC motor. Some of the manufacturers that offer this type of motor are (in alphabetical order) Baumüller, Canon, Citizen Micro, Dunkermotoren GmbH, Faulhaber GmbH, Namiki Precision Jewel, Portescap S.A. and more. Automated (or semi-automated) winding equipment is available for all of the coil configurations mentioned. **PTE**

Appendix

Index Terms: Coreless, ironless, voice coil, moving coil, basket-wound, slotless, rhombic, bell winding, and multi-saddle.

Clyde Hancock
Motor Consultants, LLC
August 3, 2020

Clyde Hancock is Chief Technical Officer of Motor Consultants, LLC, a complete design service for all types of electric motors and generators, including detailed magnetic modeling and thermal analysis using world-renowned simulation tools. Expert consulting services for associated technologies relating to rotary and linear motion control are also provided by Motor Consultants in partnership with world-leading technical associates. These services include detailed thermal analysis of electric machines and high-speed motor/generator and spindle design

www.motorconsultants.com
clyde.hancock@msn.com
Phone: 727-575-9632